Chinese Journal of Catalysis 39 (2018) 701–709 催化学报 2018年 第39卷 第4期 | www.cjcatal.org

available at www.sciencedirect.com

ScienceDirect

journal homepage: www.elsevier.com/locate/chnjc

Article (Special Issue on Environmental and Energy Catalysis)

Enhancement of UV-assisted TiO_2 degradation of ibuprofen using Fenton hybrid process at circumneutral pH

Meijuan Chen [a,b], Wei Chu [b,*], Jingzi Beiyuan [b,c], Yu Huang [d,e]

[a] *School of Human Settlements and Civil Engineering, Xi'an Jiaotong University, Xi'an 710049, Shaanxi, China*

[b] *Department of Civil and Environmental Engineering, The Hong Kong Polytechnic University, Hong Kong, China*

[c] *Centre of Sustainable Design and Environment, Faculty of Design and Environment, Technological and Higher Education Institute of Hong Kong, Hong Kong, China*

[d] *Key Lab of Aerosol Chemistry & Physics, Institute of Earth Environment, Chinese Academy of Sciences, Xi'an 710061, Shaanxi, China*

[e] *State Key Lab of Loess and Quaternary Geology (SKLLQG), Institute of Earth Environment, Chinese Academy of Sciences, Xi'an 710061, Shaanxi, China*

ARTICLE INFO

Article history:
Received 28 October 2017
Accepted 13 December 2017
Published 5 April 2018

Keywords:
Ultraviolet light
TiO_2
Fenton
Ibuprofen
Effect parameter
Kinetic model

ABSTRACT

A synergistic UV/TiO_2/Fenton (PCF) process is investigated for the degradation of ibuprofen (IBP) at circumneutral pH. The IBP decay in the PCF process is much faster than that with the conventional UV, UV/H_2O_2, Fenton, photo-Fenton, and photocatalysis processes. The kinetics analysis showed that the IBP decay follows a two-stage pseudo-first order profile, that is, a fast IBP decay (k_1) followed by a slow decay (k_2). The effects of various parameters, including initial pH level, dosage of Fenton's reagent and TiO_2, wavelength of UV irradiation, and initial IBP concentration, are evaluated. The optimum pH level, $[Fe^{2+}]_0$, $[Fe^{2+}]_0/[H_2O_2]_0$ molar ratio, and $[TiO_2]_0$ are determined to be approximately 4.22, 0.20 mmol/L, 1/40, and 1.0 g/L, respectively. The IBP decay at circumneutral pH (i.e., 6.0–8.0 for wastewater) shows the same IBP decay efficiency as that at the optimum pH of 4.22 after 30 min, which suggests that the PCF process is applicable for the treatment of wastewater in the circumneutral pH range. The $\ln k_1$ and $\ln k_2$ are observed to be linearly correlated to $1/pH_0$, $[IBP]_0$, $[H_2O_2]_0$, $[H_2O_2]_0/[Fe^{2+}]_0$ and $\ln[TiO_2]_0$. Mathematical models are therefore derived to predict the IBP decay.

1. Introduction

Pharmaceuticals and personal care products (PPCPs) are composed of a diverse group of medicines, which include prescription and over-the-counter therapeutic drugs, veterinary drugs, fragrances, cosmetics, sunscreen products, diagnostic agents, and nutraceuticals. A growing number of environmental concerns are raised owing to their biological activity, increase in usage and persistence in the environment [1]. The existence of PPCPs in aquatic organisms possibly affects human health and interferes with the balance of the ecosystem through a continuous and multigenerational exposure to the polluted water [2].

Ibuprofen (IBP), 2-(4-isobutylphenyl) propionic acid, is widely used as a nonsteroidal anti-inflammatory drug especially prescribed for the treatment of pain, fever and rheumatic

* Corresponding author. Tel: +852-2766-6075; Fax: +852-2334-6389; E-mail: cewchu@polyu.edu.hk

This work was supported by the National Natural Science Foundation of China (41503102), the China Postdoctoral Science Foundation (2015M572568), the Shaanxi Postdoctoral Science Foundation (2016BSHEDZZ35), the Hong Kong Polytechnic University (1-ZVH6, G-YBHP), and the "Hundred Talent Program" of Chinese Academy of Sciences.

DOI: 10.1016/S1872-2067(17)62916-4 | http://www.sciencedirect.com/science/journal/18722067 | Chin. J. Catal., Vol. 39, No. 4, April 2018

disorders [3]. As a result of its widespread applications, the global production of IBP has exceeded 15000 t/year [4]. IBP occupied the 17th place on the list of the most prescribed drugs in the United States [5] in 2005. In Spain, IBP was the third best-selling pharmaceutical in 2011. After application of the therapeutic dose, 15% IBP is excreted from the body in the unaltered form and is subsequently able to enter into municipal wastewater [6]. Additionally, a major contributor to the aqueous environmental concentration of the non-metabolized and metabolized forms of ibuprofen is medical waste that has not been properly managed. Many studies have shown that the removal of IBP is not appropriate through the conventional treatments employed by wastewater treatment plants because the technologies used are not sufficiently effective [7]. Previous studies have reported that in China, IBP has been detected in a reservoir at a concentration greater than 1 μg/L [8], while in the drinking water, concentrations of up to 23.3 ng/L have been reported [9]. The toxicological effect of ibuprofen metabolites originating from human and microbial activity in the aquatic environment have been reported to influence cyclooxygenase reactions, and, therefore, affect the reproduction of aquatic animals and the photosynthesis of aquatic plants [10,11]. Therefore, a number of studies on eliminating IBP from an aquatic environment have recently been carried out [12–14].

Coagulation and flocculation are poor for the elimination of IBP owing to the chemical nature and low concentration of IBP in an aqueous environment [15]. Efficient IBP removal has been achieved by adsorption and membrane treatment, but the high operational cost limits its application [16], Moreover, the adsorption and membrane treatment is simply a physical separation process, where the IBP moves from the aqueous phase to another phase as the unchanged species rather than being mineralized. Sunlight degradation, with the advantages of low cost and destruction of the chemical structure, has been estimated by A. Pal and co-workers [17]. Their results showed that sunlight degradation cannot be adopted for IBP removal in real-life application because the reaction is slow with a half-life of 9900 h. The advanced oxidation processes (AOPs) have been used for IBP degradation through the supply of active radicals (i.e., •OH, $O_2^{\bullet-}$) in the literature such as Fenton, photo-Fenton oxidation, and TiO_2 photocatalysis [6,18]. Photocatalysis is an effective process that shows good performance at neutral pH, which falls in the working pH of wastewater treatment plants and biodegradation process [7,19]. Therefore, there is no need to adjust the pH by using extra acid or alkali before and after treatment. However, the TiO_2 heterogeneous photocatalysis follows moderate first-order kinetics, for example, 60% IBP (0.24 mmol/L) degradation in 60 min [10], because the heterogeneous oxidation only occurs on the TiO_2 surface [20,21]. For comparison, the homogeneous Fenton reaction is much faster owing to the oxidation proceeds in the whole solution [22,23]. The Fenton reaction encompasses the reaction of hydrogen peroxide (H_2O_2) with Fe^{2+} under acidic conditions to form reactive oxygen species (ROS, usually •OH) that can degrade organic compounds [24]. The complex reaction mechanism of the Fenton reaction can be summarized as follows [25]:

$$Fe^{2+} + H_2O_2 \rightarrow Fe^{3+} + OH^- + {}^{\bullet}OH \quad (1)$$

However, the Fenton reaction is only competitive under acidic conditions and a pH adjustment before and after the treatment is required [14]. Considering that the water treatment at neutral pH is less harmful to the environment, it would be more appealing to develop a fast process that proceeds at the circumneutral pH level.

In this study, with the aim of integrating the advantages of both the heterogeneous photocatalysis and homogeneous photo-Fenton reactions, a combined process, namely photo/TiO_2/Fenton (PCF), was designed. The objective is to explore the IBP decay using the PCF process at circumneutral pH level. The effect of various parameters, including initial solution pH levels, dosage of Fenton's reagents and TiO_2, wavelength of UV irradiation, and initial IBP concentrations, were examined. Moreover, mathematical models were derived for the prediction of IBP degradation in the PCF process in terms of the dosage of TiO_2 and Fenton's reagents, initial IBP concentration, and initial pH levels.

2. Experimental

2.1. Chemicals and reagents

All chemicals were of analytic reagent grade, and all solvents were of HPLC grade and used as received without further purification. IBP ($C_{13}H_{18}O_2$, α-methyl-4-(isobutyl)phenylacetic acid) was purchased from Wako Pure Chemical Industries. Fenton's regents, that is, ferrous sulfate and hydrogen peroxide, were obtained from Aldrich and Riedel-de Haën, respectively. Titanium dioxide (TiO_2, Degussa P25, 80% anatase and 20% rutile) was used as the catalyst with a BET surface area of 50 m^2/g and a density of 3.85 g/cm^3. TiO_2 has an average aggregate size of 200 nm and is made up of 30 nm primary particles. The mobile phase solvent for HPLC analysis (i.e., acetonitrile) was obtained from Tedia. A resistivity of 18.2 MΩ for the distilled-deionized water was used to prepare the mobile phase and stock solution, which was obtained from a Bamstead NANOpure water treatment system (Thermo Fisher Scientific Inc., USA).

2.2. Experimental procedures

The degradation of IBP was conducted in a Rayonet RPR-200 photochemical reactor manufactured by the Southern New England Ultraviolet Co. Two phosphor-coated low-pressure mercury lamps were installed in the photoreactor. All the experiments were conducted through the following steps. First, 100 mL IBP was added into a quartz beaker (56 mm ID × 125 mm H) followed by the addition of TiO_2 with stirring for 30 min in the dark to achieve the adsorption equilibrium. The reaction was initiated by the addition of an appropriate amount of ferrous salt and hydrogen peroxide into the reactor with the simultaneous switching on of the UV lamps. The pH values were adjusted by 0.10 mol/L nitric acid and/or 0.10 mol/L sodium hydroxide whenever required. To ensure a thorough mixing, mechanical stirring was provided continuously before and during the reaction. An exact aliquot (0.5 mL) was withdrawn

from the solution at predetermined time intervals and mixed with the same amount of methanol to quench the reaction, and the samples were then filtered with 0.20 μm PTFE filters (Whatman) for further analysis.

2.3. Analytical methods

The remaining IBP was quantified by high-performance liquid chromatography (HPLC). The HPLC system comprised of a Waters 515 pump, a 20-μL-loop injection port, and a Waters 2487 absorbance detector. The IBP was separated from its intermediates by a RESTEK C18 (5 μm, 0.46 cm × 25 cm) column, and quantified at an adsorption wavelength of 220 nm. A mixture of 75% acetonitrile and 25% water was used as the mobile phase and the pH level was adjusted to 3.8 using acetic acid. Adequate degassing of the mobile phase prior to injection was performed to inhibit the generation of gas bubbles during the analysis. The flow rate of mobile phase was set at 1 mL/min. The total organic carbon (TOC) was determined by a Total Organic Carbon Analyzer (TOC-5000A, Shimadzu) equipped with an auto-sampler (ASI-5000).

3. Results and discussion

3.1. Comparative study of different processes

The following tests were carried out to evaluate the efficiency of IBP degradation at neutral pH: (1) solely UV, (2) solely H_2O_2, (3) UV/H_2O_2, (4) solely Fenton, (5) photo-Fenton (PF), (6) photocatalysis (PC), and (7) photo/catalyst/Fenton (PCF). Fig. 1(a) shows that the PCF process demonstrated a better and faster IBP degradation performance. The solely H_2O_2, solely UV and UV/H_2O_2 processes were almost inert for IBP degradation, showing 0%, 2% and 3% IBP removal, respectively. A rapid and incomplete IBP decay (about 57%) was achieved by the Fenton process in 30 min, while with the PF process the decay was improved to 66%. This positive improvement process should be attributed to the UV light, which generates additional ·OH radicals through the photo-reduction of ferric ions (Eq. 2).

$$Fe^{III}(OH)^{2+} + h\nu \rightarrow Fe^{2+} + {}^{\bullet}OH \quad (2)$$

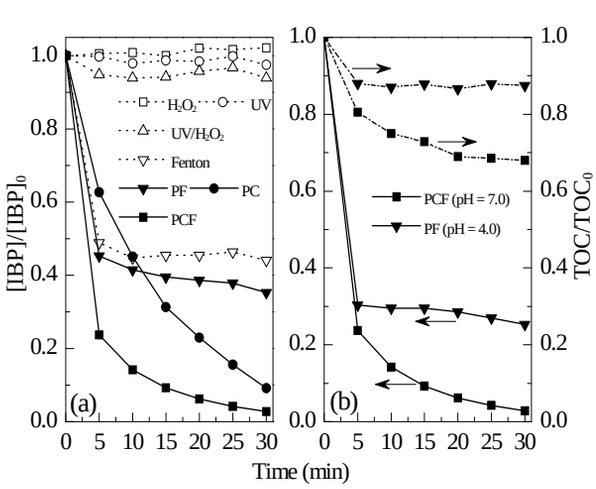

Fig. 1. (a) Comparison of different processes at neutral pH (pH = 7.0), and (b) mineralization and degradation of IBP for PCF at pH = 7.0 and for PF at pH = 4.0. Experimental conditions: $[IBP]_0$ = 0.15 mmol/L, $[Fe^{2+}]_0$ = 0.05 mmol/L, $[H_2O_2]_0$ = 0.5 mmol/L, $[TiO_2]_0$ = 0.5 g/L, UV wavelength = 350 nm, two lamps.

The overall IBP removal of 90% obtained from the PC process was higher than those from the Fenton and/or PF processes. However, the IBP removal by PC, Fenton and PF was 38%, 50% and 54% in the first 5 min, respectively. This is because the dominating heterogeneous reaction in the PC process only occurs on the TiO_2 surface, and the IBP adsorption from an aqueous solution to the TiO_2 surface is slow and is the rate-determining step. For comparison, the homogeneous Fenton and PF proceeding ubiquitously in the aqueous solution is much faster, resulting in a higher initial IBP removal rate. Nevertheless, at a later stage, the PC process shows a great advantage with a continuous IBP decay resulting from an endless supply of radicals by the PC process, whereas the Fenton and PF were almost terminated because of the exhaustion of Fenton's reagents.

Many studies have revealed that the PF process shows a better performance at an acidic pH level (between 2.0 and 4.0) [26,27]. Therefore, it is interesting to determine the performance at an acidic pH with the aim of evaluating the superiority of PCF. A pH of 4.0 was used in the PF process for comparison. The mineralization and degradation of IBP were compared between the PCF (pH = 7.0) and PF processes (pH = 4.0) as shown in Fig. 1(b). It was observed that both degradation and mineralization of IBP in PCF at a neutral pH were much better than that of PF at an acidic pH. Apparently, the rapid and continuous IBP degradation in PCF can be rationalized by its fast radical generation when integrating the advantages of homogeneous PF and heterogeneous PC. It was noted from Fig. 1(b) that TOC removal by PF was initially fast and then slowed down at the later stage, which might be attributed to the following reasons: (1) the ·OH production was slowed owing to the depletion of Fenton's reagent with an increasing reaction time; (2) although the UV photolysis in the later stage induced the IBP degradation, the intermediates formed in the first stage are resistant towards further mineralization because the oxidizing ability of UV light is insufficient for compound mineralization as reported by Zhang and coworker [28]. The better and continuous TOC removal in the PCF process indicates that complete mineralization of IBP by the PCF process is possible with a sufficient reaction time.

The kinetics analysis showed that the IBP decay through the PCF process followed a two-stage pseudo-first-order profile (Fig. 2), where a higher rate constant (k_1) at the first stage was followed by a slower rate (k_2) at the second stage. In the first stage, the faster homogeneous Fenton reaction yielded a higher k_1, which resulted in a lower remaining [IBP], and quickly accumulated intermediates at a high level in the solution. In addition, the reaction pathways of solely UV, UV/H_2O_2, PF and PC were all available in the first stage. As the reaction proceeded, the Fenton's reagents were rapidly consumed in the solution (the control experiment of the PF process showed that the IBP decay was almost terminated after 5 min); the UV and PC processes then became the remaining pathways for the further decay of IBP, and therefore, resulted in a smaller k_2.

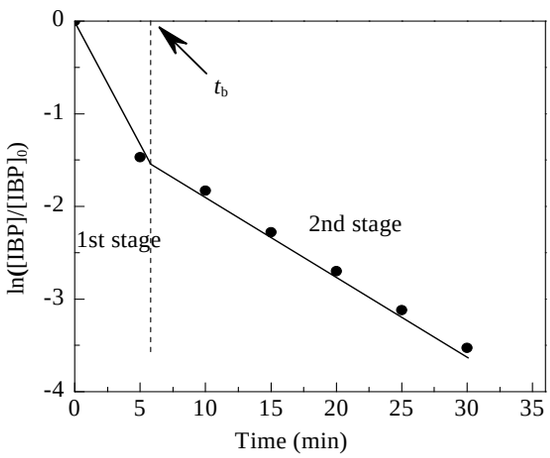

Fig. 2. Typical two-stage kinetics in the PCF process.

3.2. Effect of pH

Fig. 3 demonstrates the influence of the pH. Six pH levels were investigated for the PCF process. It was found that the IBP decay rate increased with the decline of pH. The intrinsic property of the PF sub-process is likely to be responsible for the better performance at an acidic pH (pH = 4.22) because the higher $[H^+]$ benefits the formation of ·OH and increases the output of dissolved ferrous complexes [24]. It is interesting to note that the IBP decay at circumneutral pH levels (i.e., 6.0–8.0 for wastewater) showed the same IBP decay efficiency (98.0%) at 30 min as that at an acidic pH of 4.22, despite the slower initial decay for the first 5 min ($k_{9.06} < k_{7.12} < k_{5.17} < k_{4.22}$) (Table 1). It was reported that the decay rate of organic pollutants in the PC process increased with the increment of pH in the neutral range, owing to the increase of hydroxide ions resulting in the generation of more hydroxyl radicals [29]. As a result, the IBP decay in the later stage showed the decay rate order of $k_{9.06} > k_{7.12} > k_{5.17} > k_{4.22}$ (Table 1). At an extreme alkali pH (10.98 and 11.65), the ferrous hydroxide was precipitated out from the aqueous solution and the IBP was removed by co-precipitation (if any) instead of degradation; then the PF sub-process was suppressed under these circumstances. Apparently, after combining the processes of PF and PC, the working pH level could be expanded from an acidic condition to a circumneutral pH level.

Table 1
Reaction decay rate (k, min^{-1}) values at different pH levels.

pH	Initial stage decay rate (k_1)	Later stage decay rate (k_2)
4.22	2.1037	0.1772
5.17	1.1239	0.3841
7.12	0.9997	0.3928
9.06	0.9063	0.4233

3.3. Effect of dosage of Fenton's reagents

Fenton's reagents, including ferrous salt and hydrogen peroxide, are crucial components in the PCF process. The effects of $[Fe^{2+}]_0$ and $[H_2O_2]_0$ were investigated under neutral pH for IBP decay. Fig. 4(a) shows the influence of $[H_2O_2]_0$ at $[Fe^{2+}]_0$ = 0.05 mmol/L. An increase in IBP removal was observed with the increment of $[H_2O_2]_0$. The rate improvement at high H_2O_2 dosage is proposed to arise from the following reasons. First, the generation of ·OH radicals by direct UV photolysis is likely to be the dominant rate-improving mechanism as $[H_2O_2]_0$ increases [30]. Second, the rate enhancement may partially contribute to the $[H_2O_2]$, which was suggested to be a better electron acceptor than oxygen for TiO_2 photocatalysis (see Eq. 3) [28]. This would reduce the chance of electron-holes recombination and facilitate the generation of ·OH radicals.

$$H_2O_2 + e^- \rightarrow 2^{\bullet}OH \quad (3)$$

The effect of $[Fe^{2+}]_0$ was investigated from 0.05 to 2.0 mmol/L as $[H_2O_2]_0$ was fixed at 0.5 mmol/L. As shown in Fig. 4(b), the higher the $[Fe^{2+}]_0$, the better the IBP removal. However, it is interesting to note that the IBP decay was accelerated with the increment of $[Fe^{2+}]_0$ until an optimum dosage of 0.20 mmol/L was reached, after which the reaction leveled off at higher $[Fe^{2+}]_0$. This observation is inconsistent with previous

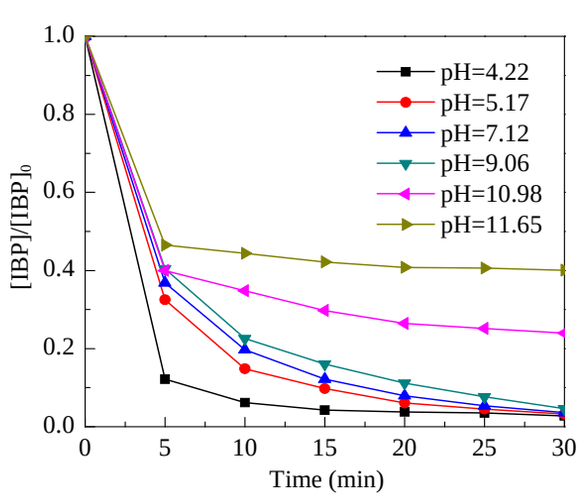

Fig. 3. Effect of pH on the degradation. Experimental conditions: $[IBP]_0$ = 0.15 mmol/L, $[Fe^{2+}]_0$ = 0.05 mmol/L, $[H_2O_2]_0$ = 0.5 mmol/L, $[TiO_2]_0$ = 0.5 g/L, UV wavelength = 350 nm, two lamps.

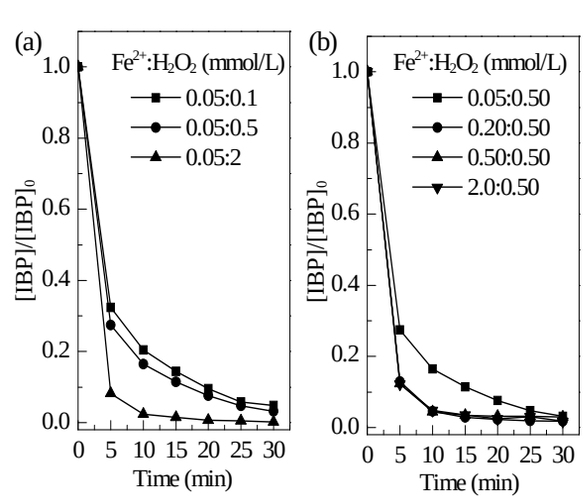

Fig. 4. Effect of the $[Fe^{2+}]/[H_2O_2]$ ratio when (a) $[Fe^{2+}]_0$ is fixed, and (b) $[H_2O_2]_0$ is fixed. Experimental conditions: $[IBP]_0$ = 0.15 mmol/L, $[TiO_2]_0$ = 0.5 g/L, UV wavelength = 350 nm, two lamps.

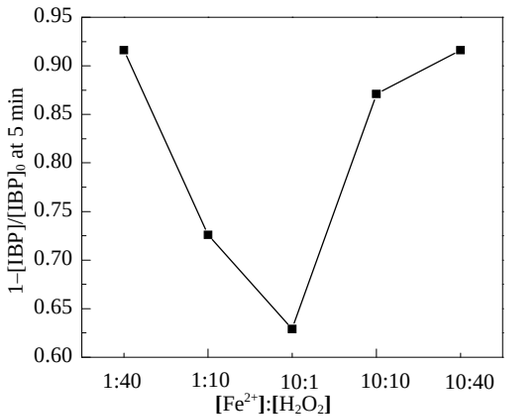

Fig. 5. Removal efficiency (1−[IBP]/[IBP]$_0$) at 5 min as a function of the [Fe^{2+}]$_0$/[H_2O_2]$_0$ molar ratio, where 1 stands for 0.05 mmol/L.

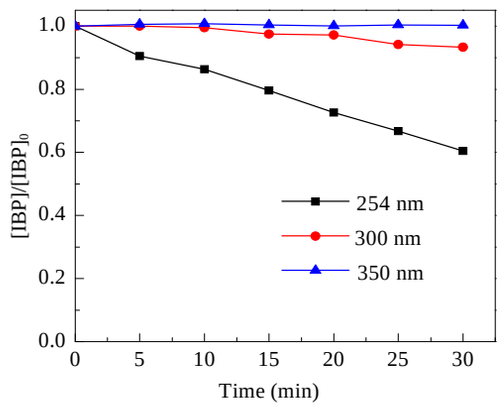

Fig. 7. UV photolysis at different wavelengths. Experimental conditions: [IBP]$_0$ = 0.15 mmol/L, two lamps.

findings [31] where the slow transformation of Fe^{2+} at lower [Fe^{2+}]$_0$ is the rate-limiting factor; if [Fe^{2+}]$_0$ is increased, the transformation of Fe^{2+} is sufficiently rapid, and it no longer acts as the rate-limiting factor. Therefore, the unlimited increase of ferrous iron does not always guarantee a beneficial effect on the PCF process.

The optimum [Fe^{2+}]$_0$/[H_2O_2]$_0$ molar ratio was identified by varying the molar ratio ranging from 1:40 to 10:40. Fig. 5 shows the decay performance of IBP at 5 min as a function of the [Fe^{2+}]$_0$/[H_2O_2]$_0$ molar ratio. In general, the closer the ratio was to 10:1, the poorer was the IBP decay. In this study, the highest IBP removal was achieved to be approximately 92% in 5 min when the [Fe^{2+}]$_0$/[H_2O_2]$_0$ ratio was either 1:40 or 10:40. Obviously, the optimum [Fe^{2+}]$_0$/[H_2O_2]$_0$ ratio should be 1:40 so as to use less ferrous iron.

3.4. *Effect of λ, [TiO_2]$_0$ and [IBP]$_0$*

Since the degradation of IBP involves the direct photolysis, photocatalysis and photo-Fenton processes, the participation of the three pathways may be varied if different UV sources (wavelengths) are applied. Fig. 6(a) shows the IBP decay through the PCF process under different UV wavelength irradiations. Three types of lamps were chosen as the UV light source, including 254, 300 and 350 nm, which represent UVC, UVB and UVA, respectively. For comparison, the IBP decay by direct photolysis (Fig. 7) and PC (Fig. 8) processes were examined under the same conditions. It was found that the IBP decay for direct photolysis increased with the decrease of UV wavelength, where direct photolysis at 254 nm gave the highest removal efficiency (39% in 30 min), followed by 300 nm (8%) and 350 nm (0%), as shown in Fig. 7. This observation can be rationalized by the fact that the lower the UV wavelength, the higher the radiation energy, which facilities the destruction of IBP through direct photolysis. Although the IBP decay performance by direct photolysis follows the descending order of UV wavelength, the use of TiO_2 at 350 nm presented almost the same IBP decay performance as UV 300 and 254 nm, as shown in Fig. 8. This observation suggests that TiO_2-induced photocatalysis at 350 nm provides a significant increment in the photocatalysis quantum yield of IBP over 300 and 254 nm [32], indicating that the application of a TiO_2 mediated photocatalyt-

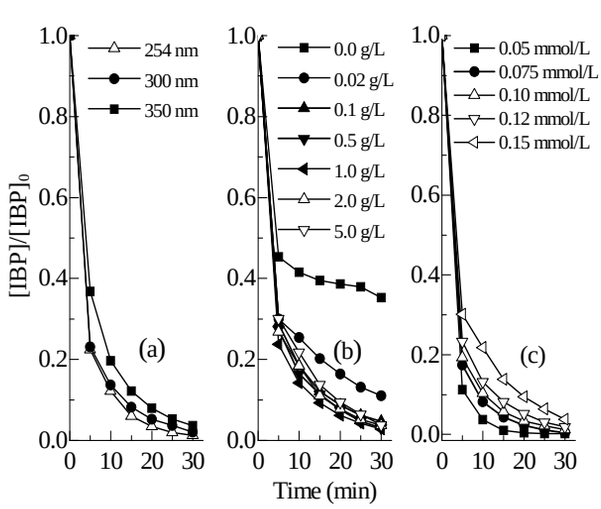

Fig. 6. Effect of (a) lamp wavelength, (b) [TiO_2]$_0$ and (c) [IBP]$_0$. Experimental conditions (except specified): [IBP]$_0$ = 0.15 mmol/L, [Fe^{2+}]$_0$ = 0.05 mmol/L, [H_2O_2]$_0$ = 0.5 mmol/L, [TiO_2]$_0$ = 0.5 g/L, pH = 7, wavelength = 350 nm, two lamps.

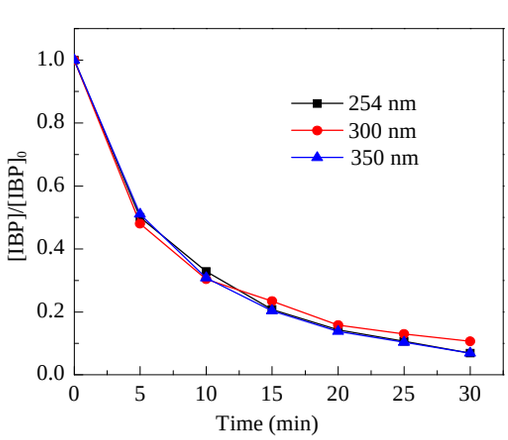

Fig. 8. IBP decay in the PC process at different wavelengths. Experimental conditions: [IBP]$_0$ = 0.15 mmol/L, [TiO_2]$_0$ = 0.5 g/L, pH$_0$ = 7, two lamps.

ic reaction is more effective under the near-UV range.

The IBP decay was found to depend slightly on the UV source in the PCF process (Fig. 6(a)), where the performance under UVC and UVB irradiation was superior to that under UVA, that is, a 2.4% and 1.7% improvement in 30 min under UVC and UVB, respectively. The differences in PCF should mainly be ascribed to the use of Fenton's reagents (i.e., H_2O_2 and Fe^{2+}) since the UV source shows an insignificant influence on the PC sub-process. The lower frequency of UV with higher irradiation energy might benefit the generation of ·OH radicals through the photo-reduction of ferric ions as depicted in Eq. 2 [18]. However, when the H_2O_2 reagent is exposed to UV light in the PCF process, the direct photolysis of H_2O_2 generates ·OH radicals and subsequently benefits the IBP degradation. It was observed in Fig. 1(a) that the direct H_2O_2 photolysis at 350 nm induced an insignificant IBP decay, because H_2O_2 has an extremely low absorption at 350 nm. The molar adsorptions of H_2O_2 at 300 and 254 nm have been reported to be higher than that at 350 nm [33], which induced the H_2O_2 photolysis for generating more ·OH radicals and slightly improved the IBP decay. In the natural environment, UVA is the dominating species among the three UV sources since both UVB and UVC are absorbed by the ozone layer in the atmosphere before they can reach the surface. This means that the use of UVA is the reasonable choice for outdoor treatment in a wastewater treatment plant despite the UVB and UVC showing a slight superiority. Therefore, lamps with an irradiation wavelength of 350 nm were selected in this study.

The effect of $[TiO_2]_0$ was investigated in terms of IBP decay under UVA irradiation at neutral pH. Fig. 6(b) shows the variation of IBP decay at six different $[TiO_2]_0$ of 0.02, 0.1, 0.5, 1.0, 2.0 and 5.0 g/L. The IBP decay was found to basically increase with the increment of TiO_2 dosage, but the reaction was retarded as $[TiO_2]_0$ became higher than 1.0 g/L. The increase in the decay rate was proposed to arise from the increase in the total surface area (or number of active sites) available for the photocatalytic reaction as the dosage of TiO_2 increased. However, when TiO_2 was in excess, the intensity of the incident UV light was attenuated because of the decreased light penetration and light scattering, which impaired the positive effect arising from the dosage increment and therefore the overall performance was reduced [32].

The efficiency of PCF as a function of the initial IBP concentration was investigated by varying $[IBP]_0$ from 0.05 to 0.15 mmol/L, and the results are presented in Fig. 6(c). It can be observed that a lower initial concentration leads to a higher removal efficiency of IBP, that is, when the $[IBP]_0$ was increased from 0.05 to 0.15 mmol/L, the IBP degradation at 5 min decreased from 88% to 70%. This observation suggested that the PCF process may be a good choice for the removal of low level contaminants like IBP (ranging from ng/L to μg/L) in wastewater in real-life applications.

3.5. Development of kinetic model

From a design point of view, the selection of reasonable dosages of TiO_2 and Fenton's reagents at certain pH levels for the PCF process is necessary to ensure a cost-effective process. Mathematical models were therefore derived for the prediction of IBP decay. Different dosages of TiO_2 and Fenton's reagents were used at different IBP concentrations under UVA irradiation. The $\ln k_1$ and $\ln k_2$ were found to be linearly correlated to $1/pH_0$, $[IBP]_0$, $[H_2O_2]_0$, $[H_2O_2]_0/[Fe^{2+}]_0$ and $\ln[TiO_2]_0$, as shown in Fig. 9(a)–(e), respectively, and the linear equations are

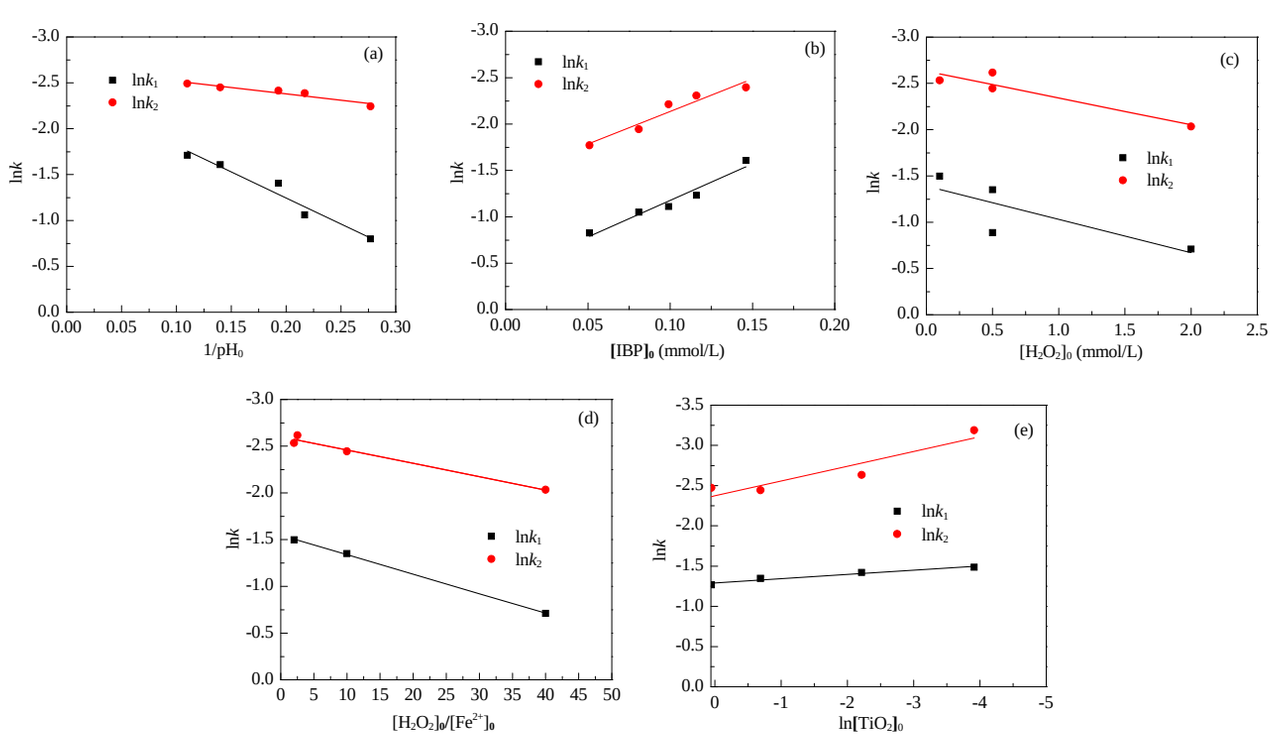

Fig. 9. Linear relation between ln*k* and (a) $1/pH_0$, (b) $[IBP]_0$, (c) $[H_2O_2]_0$, (d) $[H_2O_2]_0/[Fe^{2+}]_0$ and (e) $\ln[TiO_2]_0$.

Table 2
The linear equations of $\ln k_1$ and $\ln k_2$.

		$1/pH_0$	$[IBP]_0$	$[H_2O_2]_0$	$[H_2O_2]_0/[Fe^{2+}]_0$	$\ln[TiO_2]_0$
$\ln k_1$	a	5.710	−7.890	0.417	0.020	0.053
	b	−2.387	−0.388	−1.547	−1.547	−1.290
	r^2	0.954	0.956	0.999	0.999	0.959
$\ln k_2$	c	1.386	−7.021	0.263	0.014	0.184
	d	−2.656	−1.432	−2.561	−2.594	−2.373
	r^2	0.932	0.938	0.998	0.974	0.865

Note: $\ln k_1 = ar^2 + b$, $\ln k_2 = cr^2 + d$, and r^2 refers to $1/pH_0$, $[IBP]_0$, $[H_2O_2]_0$, $[H_2O_2]_0/[Fe^{2+}]_0$ and $\ln[TiO_2]_0$ in the linear relation of Fig. 9(a), (b), (c), (d) and (e), respectively.

summarized in Table 2. A multiple linear regression was adopted to merge the above five parameters into one simple equation. The general forms of $\ln k_1$ and $\ln k_2$ are expressed as the following equations:

$$\ln k_1 = m_1 \frac{1}{pH_0} + m_2[IBP]_0 + m_3[H_2O_2]_0 + m_4 \frac{[H_2O_2]_0}{[Fe^{2+}]_0} + m_5 \ln[TiO_2]_0 + m_6 \quad (4)$$

$$\ln k_2 = n_1 \frac{1}{pH_0} + n_2[IBP]_0 + n_3[H_2O_2]_0 + n_4 \frac{[H_2O_2]_0}{[Fe^{2+}]_0} + n_5 \ln[TiO_2]_0 + n_6 \quad (5)$$

where m_1, m_2, ..., m_6 and n_1, n_2, ..., n_6 are the process coefficients relevant to the reaction parameters. After regression analysis, the process coefficients were determined based on the initial parameters selected as shown in Eqs. 6–7.

$$\ln k_1 = 4.413 \frac{1}{pH_0} - 7.016[IBP]_0 + 1.928[H_2O_2]_0 - 0.074 \frac{[H_2O_2]_0}{[Fe^{2+}]_0} + 0.022 \ln[TiO_2]_0 - 1.27 \quad (6)$$

$$\ln k_2 = 1.275 \frac{1}{pH_0} - 7.220[IBP]_0 - 0.148[H_2O_2]_0 + 0.020 \frac{[H_2O_2]_0}{[Fe^{2+}]_0} + 0.199 \ln[TiO_2]_0 - 1.608 \quad (7)$$

It was described in Fig. 2 that the IBP decay follows two-stage pseudo-first-order kinetics in this process. The reaction kinetics in each stage could be expressed as:

$$\frac{d[IBP]}{dt} = -k\,[IBP]^n \quad (8)$$

where [IBP] is the concentration of IBP (mmol/L), t is the reaction time (min), n stands for the kinetics order that is 1 in this process, and k is the rate constant (min^{-1}).

Eq. 8 can be reformulated as:

$$\ln \frac{[IBP]}{[IBP]_0} = -k \cdot t \quad (9)$$

Thus, a two-stage model which includes a rapid phase I and a retarded phase II can be described as below:

Phase I:

$$[IBP] = [IBP]_0 e^{-k_1 \cdot t} \quad (0 \le t \le t_b) \quad (10)$$

Phase II:

$$[IBP] = [IBP]_0 e^{-k_1 \cdot t_b} e^{-k_2 \cdot (t - t_b)} (t > t_b) \quad (11)$$

where t_b is the break time to separate the two phases, since there is no significant difference of t_b under different reaction conditions owing to the very fast process, a constant t_b at 5 min was used in this study to simplify the model.

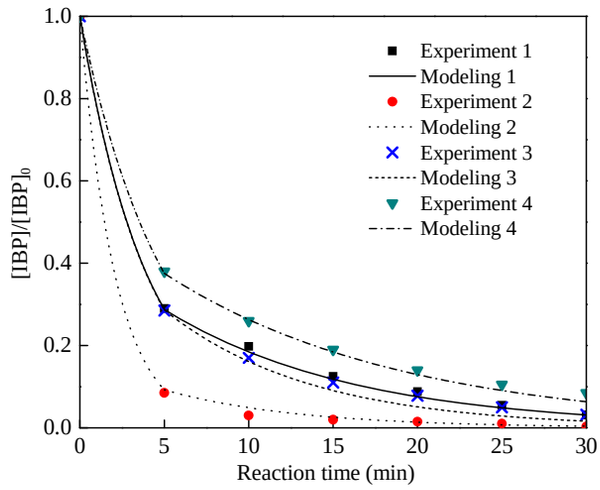

Fig. 10. Comparison between the experimental data and theoretical results.

Table 3
The experimental (EXP) conditions in Fig. 10.

EXP	pH_0	$[IBP]_0$ (mmol/L)	$[Fe^{2+}]_0$ (mmol/L)	$[H_2O_2]_0$ (mmol/L)	$[TiO_2]_0$ (g/L)
EXP1	7.13	0.134	0.05	0.5	0.501
EXP2	7.14	0.138	0.05	2	0.508
EXP3	7.14	0.138	0.05	0.5	1.998
EXP4	7.06	0.150	0.5	0.05	0.507

Fig. 10 incorporates the experimental data and the modeled data curves. The experimental (EXP) conditions are summarized in Table 3. It was found that the modeled data curves fit well to the experimental data, suggesting that the proposed models provide competent approaches for predicting the IBP decay in the PCF process.

4. Conclusions

The synergistic process of UV/TiO_2/Fenton process was investigated in this study for the degradation of IBP. The IBP decay in the PCF process is far superior to the solely UV, UV/H_2O_2, Fenton, photo-Fenton, and photocatalysis processes at neutral pH. In addition, both the degradation and mineralization of IBP by the PCF process at neutral pH are much better than those by the PF process at an acidic pH. The kinetics analysis shows that the IBP decay followed two-stage pseudo-first-order kinetics. The effect of various parameters was evaluated and optimized. The PCF process is capable for the treatment of wastewater at circumneutral pH levels between 5.17 and 9.06. In general, the higher the $[H_2O_2]_0$, the faster the IBP decay. The IBP decay accelerated with the increment of $[Fe^{2+}]_0$ until the best dosage of 0.20 mmol/L was reached. An optimum $[Fe^{2+}]_0/[H_2O_2]_0$ molar ratio at 1:40 was identified owing to the better cost-effectiveness of the selected ferrous iron dosage. The IBP decay was slightly dependent on the UV source. As a result, the application of UVA is the better choice for real-life applications. The opti-

Graphical Abstract

Chin. J. Catal., 2018, 39: 701–709 doi: 10.1016/S1872-2067(17)62916-4

Enhancement of UV-assisted TiO_2 degradation of ibuprofen using Fenton hybrid process at circumneutral pH

Meijuan Chen, Wei Chu*, Jingzi Beiyuan, Yu Huang
Xi'an Jiaotong University;
The Hong Kong Polytechnic University;
Technological and Higher Education Institute of Hong Kong;
Institute of Earth Environment, Chinese Academy of Sciences

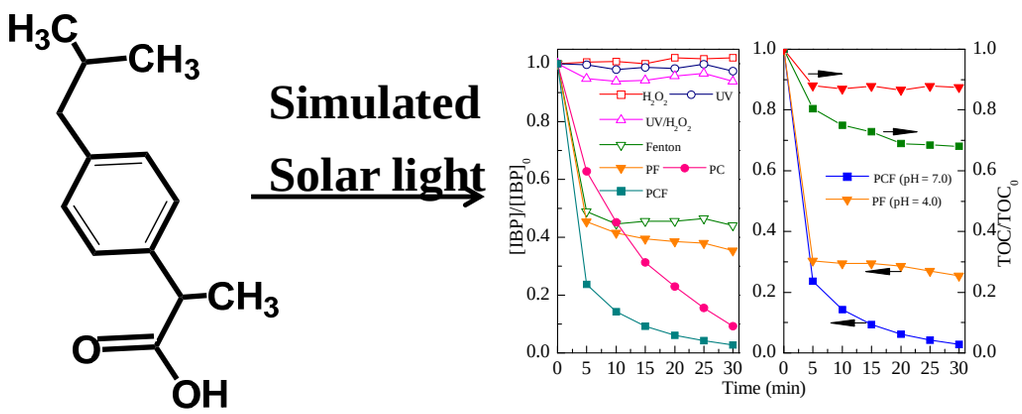

A synergistic PCF process was investigated for the degradation of ibuprofen at circumneutral pH. The IBP decay in the PCF process is much faster than that for the UV, UV/H_2O_2, Fenton, photo-Fenton and photocatalysis processes.

mum $[TiO_2]_0$ was determined to be 1.0 g/L in the PCF process, and a lower $[IBP]_0$ led to higher decay rate. The $\ln k_1$ and $\ln k_2$ were found to be linearly correlated to $1/pH_0$, $[IBP]_0$, $[H_2O_2]_0$, $[H_2O_2]_0/[Fe^{2+}]_0$ and $\ln[TiO_2]_0$. Mathematical models were therefore derived and proposed for predicting the IBP decay in terms of $1/pH_0$, $[IBP]_0$, $[H_2O_2]_0$, $[H_2O_2]_0/[Fe^{2+}]_0$ and $\ln[TiO_2]_0$. The proposed models were found to successfully predict the IBP decay in the PCF process under various reaction conditions.

References

[1] B. J. Richardson, P. K. S. Lam, M. Martin, *Mar. Pollut. Bull.*, **2005**, 50, 913–920.
[2] J. L. Liu, M. H. Wong, *Environ. Int.*, **2013**, 59, 208–224.
[3] H. R. Buser, T. Poiger, M. D. Müller, *Environ. Sci. Technol.*, **1999**, 33, 2529–2535.
[4] J. H. Zeng, B. Yang, X. P. Wang, Z. J. Li, X. W. Zhang, L. C. Lei, *Chem. Eng. J.*, **2015**, 267, 282–288.
[5] S. M. Richards, S. E. Cole, *Ecotoxicol.*, **2006**, 15, 647–656.
[6] D. Shu, J. Q. Wu, Y. B. Gong, S. Z. Li, L. L. Hu, Y. C. Yang, C. He, *Catal. Today*, **2014**, 224, 13–20.
[7] X. R. Xu, S. X. Li, X. Y. Li, J. D. Gu, F. Chen, X. Z. Li, H. B. Li, *J. Hazard. Mater.*, **2009**, 164, 527–532.
[8] X. Z. Peng, W. H. Ou, C. W. Wang, Z. F. Wang, Q. X. Huang, J. B. Jin, J. H. Tan, *Sci. Total Environ.*, **2014**, 490, 889–898.
[9] Z. H. Wen, L. Chen, X. Z. Meng, Y. P. Duan, Z. S. Zhang, E. Y. Zeng, *Sci. Total Environ.*, **2014**, 490, 987–993.
[10] A. Achilleos, E. Hapeshi, N. P. Xekoukoulotakis, D. Mantzavinos, D. Fatta-Kassinos, *Sep. Sci. Technol.*, **2010**, 45, 1564–1570.
[11] F. Pomati, A. G. Netting, D. Calamari, B. A. Neilan, *Aquat. Toxicol.*, **2004**, 67, 387–396.
[12] V. Yargeau, F. Danylo, *Water Sci. Technol.*, **2015**, 72, 491–500.
[13] M. Kim, P. Guerra, A. Shah, M. Parsa, M. Alaee, S. A. Smyth, *Water Sci. Technol.*, **2014**, 69, 2221–2229.
[14] W. Liu, Y. Y. Wang, Z. H. Ai, L. Z. Zhang, *ACS Appl. Mater. Interfaces*, **2015**, 7, 28534–28544.
[15] S. Esplugas, D. M. Bila, L. G. T. Krause, M. Dezotti, *J. Hazard. Mater.*, **2007**, 149, 631–642.
[16] F. Méndez-Arriaga, R. A. Torres-Palma, C. Pétrier, S. Esplugas, J. Gimenez, C. Pulgarin, *Water Res.*, **2009**, 43, 3984–3991.
[17] A. Pal, K. Y. H. Gin, A. Y. C. Lin, M. Reinhard, *Sci. Total Environ.*, **2010**, 408, 6062–6069.
[18] D. Q. Zhang, M. C. Wen, S. S. Zhang, P. J. Liu, W. Zhu, G. S. Li, H. X. Li, *Appl. Catal. B*, **2014**, 147 610–616.
[19] X. Wang, Y. Tang, Z. Chen, T. T. Lim, *J. Mater. Chem.*, **2012**, 22, 23149–23158.
[20] G. Lofrano, L. Rizzo, M. Grassi, V. Belgiorno, *Desalination*, **2009**, 249, 878–883.
[21] Q. J. Xiang, J. G. Yu, *Chin. J. Catal.*, **2011**, 32, 525–531.
[22] F. Méndez-Arriaga, S. Esplugas, J. Giménez, *Water Res.*, **2010**, 44, 589–595.
[23] S. J. Yuan, N. H. Liao, B. Dong, X. H. Dai, *Chin. J. Catal.*, **2016**, 37, 735–742.
[24] B. Tryba, A.W. Morawski, M. Inagaki, M. Toyoda, *Appl. Catal. B*, **2006**, 63, 215–221.
[25] E. Rott, R. Minke, U. Bali, H. Steinmetz, *Water Res.*, **2017**, 122, 345–354.
[26] B. Iurascu, I. Siminiceanu, D. Vione, M. A. Vicente, A. Gil, *Water Res.*, **2009**, 43, 1313–1322.

[27] N. Modirshahla, M. A. Behnajady, F. Ghanbary, *Dyes Pigments.*, **2007**, 73, 305–310.
[28] Q. Zhang, C. L. Li, T. Li, *Chem. Eng. J.*, **2013**, 217, 407–413.
[29] M. J. Chen, W. Chu, *J. Hazard. Mater.*, **2012**, 219–220, 183–189.
[30] C. A. Lutterbeck, M. L. Wilde, E. Baginska, C. Leder, E. L. Machado, K. Kuemmerer, *Sci. Total Environ.*, **2015**, 527–528, 232–245.
[31] Y. R. Wang, W. Chu, *Water Res.*, **2011**, 45, 3883–3889.
[32] W. Chu, C. C. Wong, *Water Res.*, **2004**, 38, 1037–1043.
[33] D. Kamel, A. Sihem, C. Halima, S. Tahar, *Desalination*, **2009**, 247, 412–422.

紫外/TiO_2/芬顿复合工艺增强在近中性pH值下对布洛芬的降解能力

陈美娟[a,b], 朱　威[b,*], 北原晶子[b,c], 黄　宇[d,e]
[a]西安交通大学人居环境与建筑工程学院, 陕西西安710049
[b]香港理工大学土木与环境工程学系, 香港
[c]香港技术高等教育学院设计与环境学院可持续设计与环境中心, 香港
[d]中国科学院地球环境研究所气溶胶化学与物理重点实验室, 陕西西安710061
[e]中国科学院地球环境研究所黄土与第四纪地质国家重点实验室(SKLLQG), 陕西西安710061

摘要: 药品及个人护理品(PPCPs)造成的潜在环境污染已引起广泛关注. 布洛芬(IBP, 2-(4-异丁基苯基)丙酸)作为苯丙酸类非甾体抗炎药物, 是一种在水环境中广泛检测到的PPCPs类物质. 水环境中的IBP主要来自制药企业排放和人体代谢物, 因IBP具有不易挥发、物理性质稳定、半衰期较长和不易被生物吸收等特点, 其在环境的残留浓度较高且污染风险大. 目前, 传统的水处理工艺并不能有效治理水中的IBP, 比如: 混凝剂和絮凝剂对IBP的去除效率低, 吸附和膜处理运行成本过高且不能矿化IBP. 近年兴起的光催化技术利用$^{\bullet}OH$和$O_2^{\bullet-}$等强氧化性活性物种降解水中有机污染物, 将其彻底矿化, 实现污染物的无害处理. 光催化技术适用于常温、常压和中性pH环境, 该环境特点与污水环境十分匹配, 适合应用. 但异质光催化通常发生在催化剂表面, 有效反应活性位少, 反应速率不够高. 相比而言, 同质芬顿反应能够均匀、快速地在整个溶液中发生反应, 但芬顿反应必须在酸性条件下才可以进行.

本文整合了异相光催化和均相光-芬顿反应的优点, 设计了紫外/TiO_2/芬顿(PCF)复合工艺, 评估了在中性pH下对典型的PPCPs布洛芬的降解效果. 对比实验结果表明, PCF复合工艺对IBP的降解速率比传统的UV, UV/H_2O_2, Fenton, 光-Fenton和光催化快得多. 动力学分析发现, IBP的降解遵循两阶段的一级反应动力学, 且速率常数$k_1 > k_2$. 本研究进一步优化了运行参数, 确定IBP降解的最佳条件为: pH = 4.2, $[Fe^{2+}]_0$ = 0.20 mmol/L, $[Fe^{2+}]_0/[H_2O_2]_0$ = 1/40, $[TiO_2]_0$ = 1.0 g/L. pH值的增加造成IBP降解速率略微降低, 但在30 min反应时间内, 中性pH (6.0–8.0)与最佳pH条件下的降解效率完全相同, 证明PCF在中性pH下进行水处理切实可行. 数据分析发现, $\ln k_1$和$\ln k_2$均与$1/pH_0$, $[IBP]_0$, $[H_2O_2]_0$, $[H_2O_2]_0/[Fe^{2+}]_0$和$\ln[TiO_2]_0$线性相关, 据此建立了IBP去除效率的数学预测模型, 通过验证发现, 动力学模型曲线与实验数据高度契合, 表明模型的有效性高.

关键词: 紫外光; 二氧化钛; 芬顿; 布洛芬; 影响参数; 动力学模型

收稿日期: 2017-10-28. 接受日期: 2017-12-13. 出版日期: 2018-04-05.
*通讯联系人. 电话: +852-2766-6075; 传真: +852-2334-6389; 电子信箱: cewchu@polyu.edu.hk
基金来源: 国家自然科学基金(41503102); 中国博士后科学基金(2015M572568); 陕西博士后科学基金(2016BSHEDZZ35); 香港理工大学基金(1-ZVH6, G-YBHP); 中国科学院“百人计划”.
本文的英文电子版由Elsevier出版社在ScienceDirect上出版(http://www.sciencedirect.com/science/journal/18722067).